Carbon Dioxide Concentration for Manned Spacecraft Using a Molten Carbonate Electrochemical Cell

A high-temperature molten carbonate electrochemical cell has been tested for use as a carbon dioxide concentrator in a manned spacecraft. Carbon dioxide is removed from a stream of cabin air supplied to the cathode of the bench scale cell. It is then concentrated through the molten carbonate electrolyte to the anode. The anode is fed either hydrogen (energy producer) or nitrogen (substance producer). Performance variation with gas flow rate, cell temperature, carbon dioxide partial pressure, and current are presented and analyzed.

J. WINNICK and H. TOGHIANI

University of Missouri
Columbia, MO 65211

and P. D. QUATTRONE

NASA Ames Research Center
Moffett Field, CA 94035

SCOPE

Carbon dioxide concentration is a fundamental process that must be provided in a manned spacecraft. Expendable absorption processes (LiOH cannisters) have been utilized in the Mercury, Gemini and Apollo manned missions and will be utilized for the early Space Shuttle flights. Regenerable techniques are required for longer duration manned missions in order to effect weight savings. Skylab, for example, utilized a molecular sieve/silica gel adsorption process.

The major emphasis on future regenerative CO_2 removal processes is maintenance of low ($\leq$500 Pa) space cabin CO_2 partial pressures for biomedical reasons as well as weight savings. The aqueous carbonate electrochemical CO_2 concentrator (EDC) (Life Systems, 1979) has been developed for future applications and offers many trade-off advantages over other processes in this regard. Investigative studies, however, have indicated that performance of the aqueous electrolytes in the EDC is limited by relative humidity (Life Systems, 1979). Since some future applications are envisioned in which the control of cabin humidity levels is essentially non-existent, relative humidities of near 0% to near 100% may exist.

The application of the aqueous carbon dioxide concentrator suggests use of a similar device utilizing a molten salt as the electrolyte. Operation of a concentrator using a molten salt electrolyte offers the advantage of being insensitive to relative humidity. The molten salt electrolyte also possesses a more highly concentrated ionic field, yielding high thermal and electrical conductivities for the electrolyte (Kerridge, 1975). High conductance is a desirable property. At higher temperatures, the kinetics of both electrodic reactions are enhanced.

Use of noble metal electrodes in the aqueous cell permits high power and current density and long cell duration. In a high temperature cell, the need for noble metal electrodes is reduced since non-noble metals are available which, at cell operating temperatures, are catalytically active enough for both cathodic and anodic reactions.

An electrochemical cell utilizing a molten carbonate electrolyte is an obvious extension to higher temperature from the aqueous concentrator. While these devices have been used for fuel cells (e.g., Institute of Gas Technology, 1976), they have not been tested as carbon dioxide concentrators. To determine system response to variations in process parameters, a series of tests have been conducted.

CONCLUSIONS AND SIGNIFICANCE

A carbon dioxide concentrator has been assembled from molten carbonate fuel cell components. Testing has been carried out at conditions typical for maintaining a manned-spacecraft cabin. Although the current densities are somewhat lower than obtained in fuel cells the process works successfully. The significant difference in operating conditions is the low carbon dioxide pressure in the oxidant. Improved mass transfer at the cathode in future tests should prove beneficial.

The process can operate either as an energy producer (similar to a fuel cell) or as a substrate producer (a true concentration cell). Tests show either mode is feasible. Mission parameters (e.g., cost of hydrogen vs. electrical energy) would determine which is the more desirable.

The results indicate the process will operate under less restrictive humidity conditions than will the aqueous electrochemical concentrator (Life Systems, 1979). Furthermore, it appears to be able to operate at higher current densities (thus requiring less total contact area) with similar higher efficiencies.

INTRODUCTION

The average man requires some 0.83 kg of oxygen per day and generates approximately 1.0 kg of carbon dioxide per day (Sribnik and Dean, 1971). In manned spacecraft missions, the expense of maintaining separate oxygen supply and carbon dioxide removal systems direct attention to a dual performance system, one which not only removes carbon dioxide but also generates a concentrated stream for subsequent treatment for oxygen recovery. An early system which performed this task was the aqueous alkaline carbon dioxide concentrator (Lin and Winnick, 1974; Winnick, et al., 1974; Abdel Salam and Winnick, 1976; Life Systems, Inc., 1979).

J. Winnick is presently at Georgia Institute of Technology, Atlanta, Georgia 30332.

0001-1541-82-5100-0103-$2.00

The aqueous carbon dioxide concentrator using cesium carbonate as the electrolyte performed successfully with high relative humidities (≥60% RH). Below 60% relative humidity, drying of the electrolyte induces $CsHCO_3$ precipitation at the anode which in turn allows hydrogen crossover to the cathode to take place.

Although control of humidity is possible, it is not desirable since such control not only increases capital and operating costs, but also increases total system equivalent weight. Thus, it is desirable to use an electrolyte which can function over a broad range of relative humidity. One such electrolyte is tetramethyl ammonium carbonate. Its solution having a lower vapor pressure than a cesium carbonate solution, permits cell operation at relative humidities as low as 35% (Abdel Salam and Winnick, 1976).

To alleviate performance problems associated with the aqueous concentrator's dependence on relative humidity, a system similar to the molten carbonate fuel cell was developed. This electrochemical concentrator, operating at elevated temperature (above 673°K), utilizes a molten carbonate electrolyte (e.g., 62 mol % Li_2CO_3, 38 mole % K_2CO_3, binary eutectic) contained in a porous, non-conductive support matrix (e.g., lithium aluminum oxide, $LiAlO_2$).

THEORY

Typically, the average concentration of carbon dioxide in a manned spacecraft must be maintained at less than 400 Pa P_{CO_2} (Abdel Salam and Winnick, 1976). The cabin air is the oxidant which is supplied to the carbon dioxide concentrator cathode. This air stream has a much lower carbon dioxide concentration than the oxidant feed for the molten carbonate fuel cell cathode (typically, 30% CO_2/70% air). The anode in the fuel cell is supplied fuel gas of hydrogen content from 15 to 50%.

The mechanisms for the cathodic and anodic reactions have not been completely determined, although a variety of mechanisms have been hypothesized. Most investigators, however, agree that the overall cathodic reaction is most certainly (Institute of Gas Technology, 1976):

$$CO_2 + 1/2O_2 + 2e^- \rightarrow CO_3^{2-} \tag{1}$$

Hydrogen Mode

If pure hydrogen is supplied as fuel to the anode of the concentrator, the system will operate in the fuel cell mode (or hydrogen mode), producing power but concurrently concentrating carbon dioxide from the cathode to the anode (Figure 1). Operating in the hydrogen mode, the anode functions and responds precisely as does the molten carbonate fuel cell anode. The introduction of hydrogen as a fuel at the anode causes the production of acidic species via the reaction:

$$H_2 + CO_3^{2-} \rightarrow H_2O + CO_2 + 2e^- \tag{2}$$

However, with this mode of operation, there is not only an electrochemical reaction, but also a chemical reaction, the water-gas shift reaction:

$$CO_2 + H_2 \rightleftarrows CO + H_2O \tag{3}$$

The overall reaction governing the open-circuit potential for the concentrator operating in the hydrogen mode is:

$$H_2 + 1/2O_2 \rightarrow H_2O \tag{4}$$

The equilibrium potential, E, is a function of the electrical potential, E^0, for the overall reaction. It can be calculated from the Gibbs free energy of the overall reaction and the activities of the gas components taking part in the electrochemical anodic and cathodic reactions through the Nernst equation.

The equilibrium potential for the anodic reaction, assuming the activity of the carbonate anion to be unity, is given by:

$$E_A = E_A^0 + \frac{RT}{2F} \ln \left[\frac{a_{H_2O} a_{CO_2}}{a_{H_2}}\right]_A \tag{5}$$

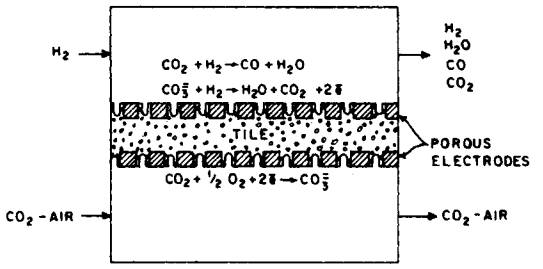

Figure 1. Electrochemical CO_2 concentrating cell in hydrogen mode.

For the cathode, the activity of the carbonate anion is again assumed to be unity, and thus, the equilibrium potential governing the reaction is:

$$E_C = E_C^0 + \frac{RT}{2F} \ln [a_{CO_2} a_{O_2}^{1/2}]_C \tag{6}$$

The overall equilibrium potential for the system is simply the difference between the cathodic and the anodic equilibrium potentials. It is written as a function of the standard electrode potential, E^0, and the Nernst terms associated with electrodic reactions:

$$E = E_C - E_A \tag{7}$$

$$E = E^0 + \frac{RT}{2F} \ln \frac{(a_{CO_2} a_{O_2}^{1/2})_C}{\left[\frac{a_{H_2O} a_{CO_2}}{a_{H_2}}\right]_A} \tag{8}$$

The operating cell voltage will differ from the equilibrium voltage due to the voltage driving forces necessary to maintain current flow. While these driving forces, or "overpotentials" are reported in Results, no analysis is presented.

Driven Mode

If an external power supply is added to the system in order to drive the cell reaction, the system functions as a concentrator in the classical sense (Figure 2). In the driven or nitrogen mode, an inert gas such as nitrogen is supplied to the anode to function as the product carrier. The cathodic reaction remains the same as for the fuel cell mode. However, the reaction at the anode becomes simply the reverse of the cathodic reaction:

$$2e^- + CO_2 + 1/2O_2 \underset{\text{Anodic}}{\overset{\text{Cathodic}}{\rightleftarrows}} CO_3^{2-} \tag{9}$$

The dependence of the potential on the activities of oxygen, carbon dioxide, and carbonate anion may be described by the Nernst equation.

$$E = E^0 + \frac{RT}{2F}\left\{\ln\left[\frac{a_{CO_2} a_{O_2}^{1/2}}{a_{CO_3^{2-}}}\right]_C + \ln\left[\frac{a_{CO_3^{2-}}}{a_{CO_2} a_{O_2}^{1/2}}\right]_A\right\} \tag{10}$$

where E^0 is zero. Assuming $(a_{CO_3^{2-}})_C = (a_{CO_3^{2-}})_A = 1$, the equation reduces to:

$$E = \frac{RT}{2F} \ln \left[\frac{(a_{O_2}^{1/2} a_{CO_2})_C}{(a_{O_2}^{1/2} a_{CO_2})_A}\right] \tag{11}$$

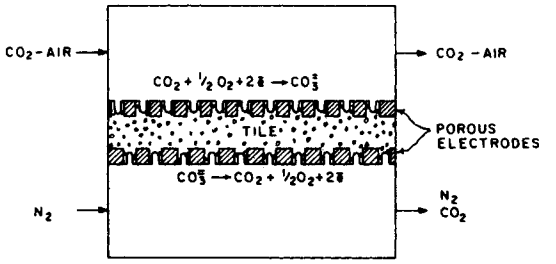

Figure 2. Electrochemical CO_2 concentrating cell in nitrogen mode.

Examination of the cathodic and anodic reactions reveals that for every two Faradays of electrical current supplied by the concentrator operating in the hydrogen mode, or to the concentrator operating in the nitrogen mode, one mole of carbonate anion must be transported from the cathode through the electrolyte to the anode.

While the anodic process in the hydrogen mode is identical with that in the fuel cell, this is not the case in the driven mode. The characteristics of the anodic oxidation of carbonate anions, with subsequent removal of the gaseous products must be determined.

EXPERIMENTAL

A test of an elevated temperature carbon dioxide concentrator utilizing a molten carbonate electrolyte requires apparatus similar to that for a fuel cell test. Basic needs of both systems are an electrochemical cell, a measurement system, gas supply, and a furnace.

Cell Design

The electrochemical cell itself consists of three main components: the cell housing, the electrodes and the electrolytic tile. The cell housing (Figure 3) is made of 316 stainless steel. Each chamber is equipped with an inlet and outlet port, to allow passage of reactant and product gases to and from the reaction site, respectively. Each chamber is also equipped with a thermocouple port to allow the temperature to be monitored. The outside edge of the cell housing, the wet seal area, is very susceptible to corrosion in the molten carbonate environment. IGT (Institute of Gas Technology, 1976) has found that the chromium in stainless steel will oxidize under normal operating conditions to form chromium oxide, which will in turn react with lithium carbonate present in the tile by the reaction:

$$Li_2CO_{3(l)} + Cr_2O_{3(s)} \rightarrow 2LiCrO_{2(s)} + CO_{2(g)} \qquad (12)$$

It is desirable to reduce or eliminate the possibility of this reaction occuring since lithium chromium oxide increases the corrosion of the housing wet seal area. To avoid excessive corrosion, the wet seal can be flame-sprayed (Swaroop et al., 1978) or painted with aluminum. Heating the cell housing for thirty minutes at 1273K under a nitrogen atmosphere allows the formation of a diffused layer of aluminum and stainless steel. During the cooling process, performed under an air atmosphere, the aluminum will oxidize to aluminum oxide (Al_2O_3). During cell operation, the alumina will react with lithium carbonate from the electrolyte to provide a corrosion-protection layer of lithium aluminum oxide.

$$Li_2CO_3 + Al_2O_3 \rightarrow 2LiAlO_2 + CO_2 \qquad (13)$$

Electrode oxidation in molten carbonate cells increases the resistance

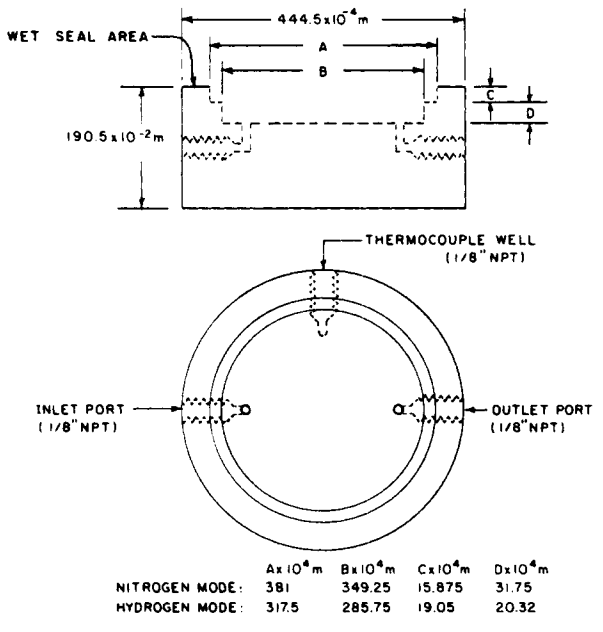

	Ax10⁴m	Bx10⁴m	Cx10⁴m	Dx10⁴m
NITROGEN MODE:	381	349.25	15.875	31.75
HYDROGEN MODE:	317.5	285.75	19.05	20.32

Figure 3. Cell design showing different dimensions on one compartment.

polarization. Due to the high operating temperatures required, electrodes must be either highly resistant to corrosion or have the ability to form a stable conductive oxide surface in order to provide an electron transfer path.

Initially, noble metals such as gold seemed to be the ideal choice since such metals are relatively immune to oxidation and corrosion. However, due to the high cost incurred using such metals, an electrode made of a less expensive material which forms a stable conductive oxide surface appears desirable. A prime candidate for both cathode and anode is a transition metal such as nickel.

Ksenzhek (1966) states "As the electrode porosity increases, the effective conductance of the gaseous and liquid phases combined will likewise increase because of the increased quantity of these phases in the pores. The kinetic conductance will decrease in the process since the total amount of solid phase present, and the related surface area also decreases." Thus, in order to achieve high current efficiencies, the desireable electrodes need to provide larger surface area (reaction area).

Candidates meeting this requirement were prepared by Gould, Inc., Cleveland, Ohio. For hydrogen mode operation experiments, porous electrodes of pure nickel were used 7.6×10^{-4} m thick and 80% porous, area of 7.92×10^{-4} m^2. The nickel cathode, when subjected to the operating environment, will be oxidized to nickel oxide, NiO. The anode electrode retains its initial state.

The addition of chromium to the electrode material served to effectively inhibit the occurrence of structural changes that could possibly take place in the anode chamber. For nitrogen mode operation experiments, the electrodes, composed of 90% Ni and 10% Cr, were 7.6×10^{-4} m thick with an average pore size of 10 μm and porosity of 83%. Both cathode and anode readily convert to nickel oxide under cell operating conditions.

The reaction site in both cathodic and anodic chambers is the electrode-electrolyte interface. Cell performance is greatly enhanced when there is maximum contact area between the electrode and the electrolytic tile. This contact can be increased through the use of an electrode support which also functions as a current collector.

A sinusoidally shaped flow channelizer (area of 2.9×10^{-4} m^2) made of stainless was incorporated into the hydrogen mode apparatus to serve as both the current collector and electrode support. A perforated stainless steel current collector (area of 9.1×10^{-4} m^2) was introduced into the nitrogen mode apparatus to serve as the electrode support. The sinusoidally shaped current collector has a smaller surface area in contact with the electrode than the perforated stainless steel current collector. Therefore, it allows a larger portion of the electrode surface to be available as a reaction site.

Generally, the electrolyte used in cell tests was a binary alkali carbonate eutectic (62 mode % Li_2CO_3, 38 mol % K_2CO_3), contained in a porous, non-conductive, and inert matrix of lithium aluminate ($LiAlO_2$) particles. The primary function of this electrolyte-matrix combination, called the electrolytic tile, in an electrochemical concentration cell is to supply a sufficient amount of electrolyte to wet the electrode surface. At cell operating temperatures, the electrolyte becomes molten and the lithium aluminate support matrix serves to retain the molten carbonates.

For use in an electrochemical concentrator, certain tile properties are desirable. The tile should possess a relatively high density (>95% of the theoretical), since during operation, the molten carbonates (melting point 761°K) fill in void space present in the tile. The matrix particles must provide sufficient capillarity to prevent flooding of the electrode pores, resulting in poor performance (Institute of Gas Technology, 1979). The faces of the tile must be parallel to avoid leakage of process gas through the wet seal area. Since a thicker tile requires more time to reach steady-state, and increases the ohmic resistance, it is desired to manufacture tiles as thin as possible.

Tiles used for hydrogen mode operation were prepared by Argonne National Laboratory by hot pressing (27 to 40 MPa, 750°K), a mixture of 45% γ-lithium aluminate and 55% binary carbonate eutectic (62 mole % Li_2CO_3) by weight (Argonne National Laboratory, 1977). The electrolytic tiles used during nitrogen mode operation were prepared by the same technique, with the exception of 50% by weight β-lithium aluminate being used instead of 45% by weight γ-lithium aluminate.

Measurement System

The process flowsheet for the hydrogen mode tests is shown in Figure 4. The nitrogen mode flowsheet is identical with the exception that the catalytic reactor and recycle pump are excluded from the anode stream.

A non-dispersive infrared (IR) analyzer (Beckman Model 864) is used to monitor the carbon dioxide concentration in both anode and cathode streams. This analyzer measures concentration of carbon dioxide in the ranges of 0.0 to 0.5% and 0.0 to 2.5% by volume. Measurements are precise to within ±1% of the full-scale value.

The largest problem encountered in hydrogen mode operation is measurement of carbon dioxide concentrations in the anode gas stream. Due

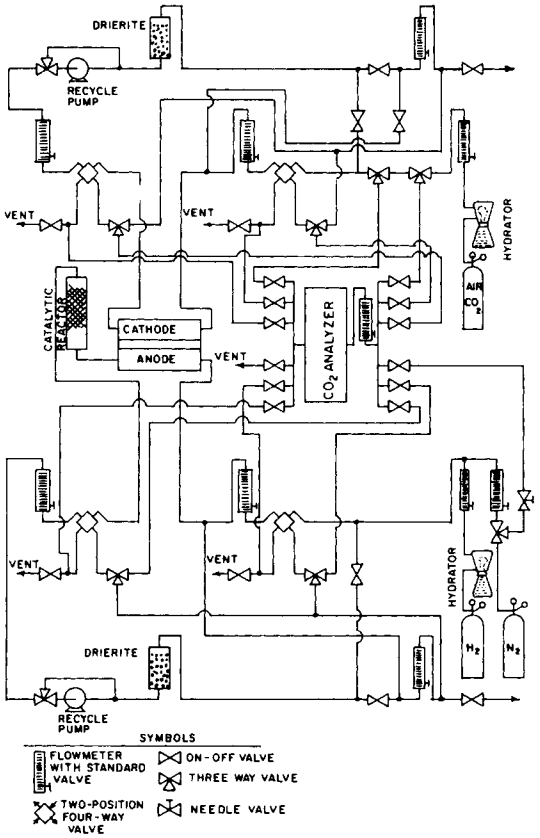

Figure 4. Flow sheet for hydrogen mode.

to the water-gas shift reaction, the reaction products at the anode outlet are essentially carbon monoxide and water. Carbon monoxide cannot be measured by the CO_2 analyzer. If the water could be isolated and weighed, the total carbon oxides concentration could be estimated by knowledge of the stoichiometric reaction and equilibrium constant.

An alternative to isolating the water vapor was to introduce a catalyst in the anode stream to reverse the water-gas shift reaction. A low temperature carbon monoxide conversion catalyst, C18-HC (United Catalyst, Inc., UCI) is used to convert the carbon monoxide and water in the anode stream to carbon dioxide and hydrogen. The carbon dioxide concentration is then measured directly by the IR analyzer.

To check for the presence of any carbon monoxide in the anode product stream during hydrogen mode operation, a carbon monoxide analyzer is employed. The analyzer can detect carbon monoxide at concentrations as low as one PPM. The detector can also be used to check for the presence of any carbon monoxide due to crossover of hydrogen to the cathode or use of humid air.

A four channel multiplexer recording system was used to continuously monitor the voltage, the temperature of the cell and carbon dioxide concentration measured in the IR analyzer. Current, voltage, and temperature of the cell were also checked using two digital multimeters (Simpson Model 460-3A).

Use of a decade resistance allows measurement of the voltage-current curve by changing the external resistance of the cell.

Furnace

The furnace, which houses the cell during operation, is made from mild-steel plates and is constructed as illustrated in Figure 5. Two layers of asbestos fiber insulation are used to insulate the furnace. Ceramic lava blocks are used on both the top and bottom of the cell in the furnace to prevent short-circuiting of the cell by the heaters. The heaters are made of mild-steel plates which have heating elements (fire-rods) placed inside them. To prevent or reduce primary leakage through the cell housing-tile interface, the cell is immobilized by applying pressure through a pneumatic cylinder. The cylinder is attached to a ram which in turn is in contact with the steel pressure plate. Conduction of heat through the plate to the ram and ultimately to the pneumatic cylinder outside the furnace could cause damage to the pneumatic cylinder's oil seals. Thus, a fan is incorporated into the system to dissipate this conducted heat and to cool the pneumatic cylinder.

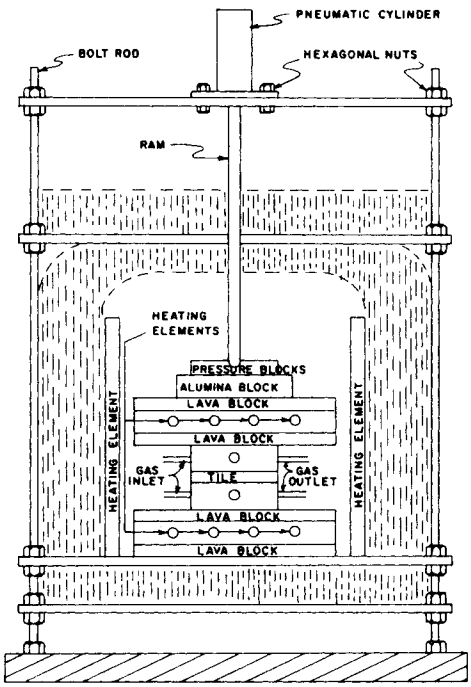

Figure 5. Schematic diagram of the furnace housing the assembled cell.

OPERATION

The assembled cell was placed in the furnace and the holding pressure applied by the pneumatic cylinder. The holding pressure ranged from 0.0 to 6.9 kPa. The furnace was heated at a rate of 50°K to 100°K per hour to operating temperature.

In early hydrogen-mode runs, nitrogen was sent through both cathode and anode during the entire heating period. A few hours after the electrolyte melting point was reached, hydrogen was started through the anode and process air was sent through the cathode. In subsequent runs, hydrogen was sent through the anode and process air was sent through the cathode during the entire heating period. An improvement in open-circuit voltage was noted.

In the nitrogen mode, no gas was sent through either anode or cathode before the melting point of the carbonate eutectic was reached (761°K). At the melting point, process air was started through the cathode and nitrogen, the inert gas carrier, was sent through the anode.

For both operational modes, system measurements were begun after approximately one day of open-circuit operation. The system was allowed to stabilize between approximately three to 12 hours after change of any process variables (cathode gas composition, gas flow rate, or cell operating temperature).

The carbon dioxide removal rate was measured and current and removal efficiencies calculated for discrete values of current density in the range of 19. to 294. A/m^2; P_{CO_2} in the range of 0.4 to 2.0 kPa; and process air volumetric flow rates between 5.5×10^{-3} and 11.6×10^{-3} m^3/h (measured at ambient temperature). The hydrogen flow rate for the fuel cell mode was in the range of 1.0×10^{-3} to 2.0×10^{-3} m^3/h. The majority of test runs were made using bottled dry gases. However, humidified gases with P_{H_2O} up to 2.2 kPa were supplied to the system for a hydrogen mode run using 2.0 kPa P_{CO_2}.

The nitrogen flow rate was controlled at 12×10^{-3} m^3/h when the system was functioning as a substance producer.

RESULTS

The ratio of the moles of carbon dioxide removed to the theoretical moles that could be removed by two Faradays of electricity is called the current efficiency. Current efficiency is related to the

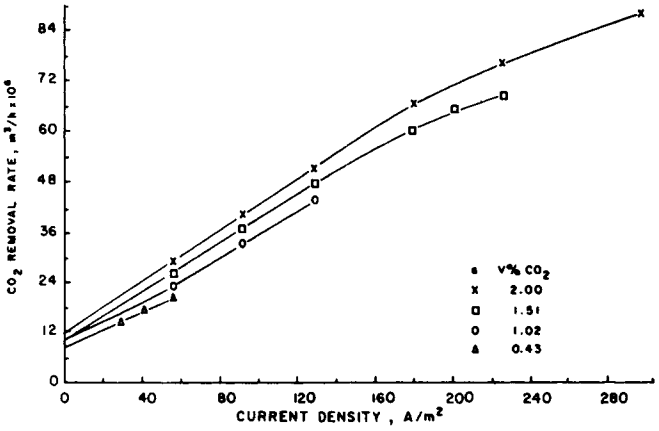

TEMPERATURE: 843 K
FLOWRATES: 5.52x10^-3 m3/h FOR CATHODE AND 1.98x10^-3 m3/h FOR ANODE

Figure 6. Carbon dioxide removal rate as a function of current density.

carbon dioxide removal rate and current by:

$$E_{ff_1} = \frac{7.9 \times 10^{-6} N_{CO_2}}{I} \tag{14}$$

where N_{CO_2} is in at 298°K and I is amps.

The removal efficiency is the percent of the inlet oxidant carbon dioxide removed.

Hydrogen Mode

Effect of Current Density. The effect of current density on the cell performance characteristics of removal rate, removal efficiency, and current efficiency are shown in Figures 6, 7, and 8.

Both the removal rate and removal efficiency increase nearly linearly with increasing current density. A decay in current efficiency as the current rises is observed.

Current efficiencies in excess of 100%, are noted based on inlet CO_2 concentration. According to Stepanov and Trunov, (1966), this is caused by carbon dioxide utilization at open-circuit. There should be a side reaction taking place. This secondary chemical reaction is:

$$CO_2 + M_2O \rightarrow M_2CO_3 \tag{15}$$

where CO_2 is utilized in the absence of current. In this reaction, oxygen is not utilized and carbon dioxide transport is dependent upon the rate of supply of M_2O through the reaction zone from the electrolyte surface. Further, there may be some transfer of CO_2 as oxalate anion, $C_2O_4^{2-}$ (Vogel, et al., 1980). This mechanism would transfer one mole of CO_2 for each Faraday, or twice the current efficiency of the primary reaction.

It is hypothesized, since only hydrogen is supplied to the anode,

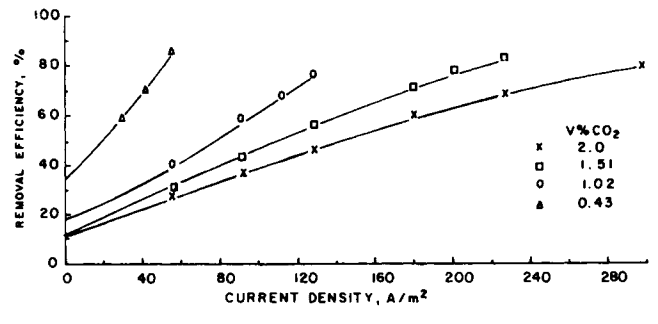

TEMPERATURE 843 K
FLOWRATES: 5.52x10^-3 m3/h FOR CATHODE AND 1.98x10^-3 m3/h FOR ANODE

Figure 7. Effect of current density on removal efficiency.

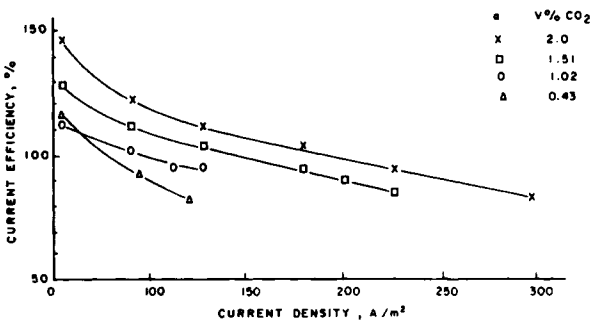

TEMPERATURE: 843 K
CATHODIC FLOWRATE: 5.52x10^-3 m3/h FOR 2%, 1.51% AND 1.02% CO2 AND 11.22x10^-3 m3/h FOR 0.43% CO2
ANODIC FLOWRATE: 1.98x10^-3 m3/h HYDROGEN

Figure 8. Effect of current density on current efficiency.

that the equilibrium of the dissociation reaction:

$$M_2CO_3 \rightleftarrows M_2O + CO_2 \tag{16}$$

may be responsible for the generation of carbon dioxide at open-circuit. The activity of the oxide ion (O^{2-}) in the molten electrolyte varies inversely with the CO_2 partial pressure above the molten carbonate. The system will attempt to establish equilibrium, consuming carbonate anions and producing oxide ions and carbon dioxide until the equilibria criteria are met (when the partial pressure of carbon dioxide in the anode chamber is either equal to or greater than the equilibrium dissociation pressure defined by the equilibrium of Eq. 16 (Degobert and Bloch, 1962).

Effect of Air-CO_2 Velocity and P_{CO_2}. Comparison of the effect of air velocity and P_{CO_2} on various electrochemical properties is depicted graphically in Figures 9 and 10. Increasing the air velocity at constant current density does not cause a significant increase in the removal rate of carbon dioxide. However, an increase in P_{CO_2} does cause a significant increase in the rate of removal, especially at higher current densities. The rate of removal exhibits a faster increase in the low P_{CO_2} region than in the higher P_{CO_2} region. This decline in increase of removal rate with increasing P_{CO_2} is caused by a change in the controlling mechanism. It has been determined in an independent study (Winnick and Ross, 1981) that, at zero utilization (i.e., very high gas flow rates), the cathodic reaction rate is nearly independent of CO_2 pressure. This same behavior is observed at high CO_2 pressures and (relatively) low currents.

Increasing the air-CO_2 velocity affects the cell voltage, but only to a limited degree. As observed in Figure 9, the voltage increases by 52 mV as the flow rate of the air-CO_2 mixture is increased 3.6×10^{-3} to 11.6×10^{-3} m^3/h for 1.5/V% CO_2. Increasing the flow rate above 11.6×10^{-3} m^3/h did not increase the cell voltage.

Effect of Hydrogen Flow Rate. Presented in Figure 11 is the effect of current density on the cell potential at two hydrogen flow

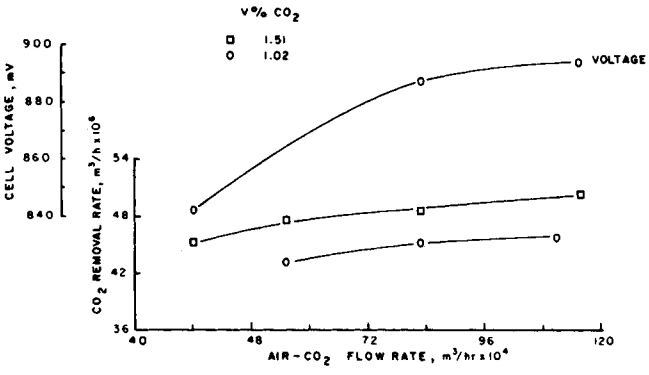

TEMPERATURE 843°K
ANODE FLOWRATE 1.98 x 10^-3 m3/h

Figure 9. Effect of air-CO_2 flow rate on CO_2 removal rate and cell voltage at 126 A/m^2.

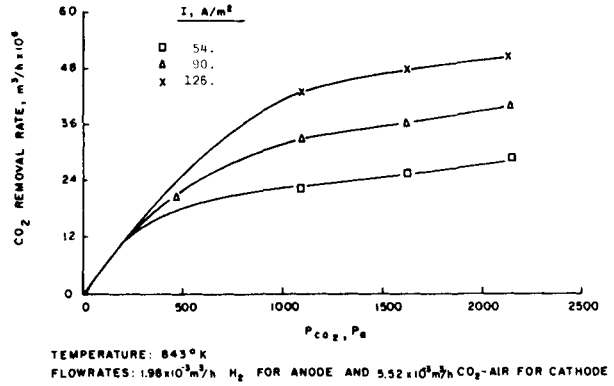

Figure 10. Effect of P_{CO_2} on removal rate.

rates. At the higher hydrogen flow rate, the cell voltage is greater for all of the inlet compositions (2%, 1.51%, 1.02%, and 0.43%). The increase in voltage is due to increased mass transfer of hydrogen to the electrode and increased product removal.

As expected, at constant cathode and anode flow rates, improved cell voltages are observed at the concentration of the carbon dioxide in the cathode inlet is increased.

Effect of Open-Circuit Operation on Cell. The response of cell potential to applied current density as a function of time is shown in Figure 12. As the applied polarization current is removed and the system returns to open-circuit operation, the cell potential returns to its rest potential. The return of the potential to its original state is an indication of the electrode stability during cycling.

Effect of Temperature on Cell Performance. The effect of increasing the temperature on cell performance for 2% by volume carbon dioxide at 126 A/m^2 is depicted graphically in Figure 13. There is a significant increase in the carbon dioxide removal efficiency (46–60%), an increase of 47 mV in the cell voltage and a decrease of 29 mV in the open-circuit potential, as the temperature is increased from 843°K to 963°K.

The increase in removal efficiency is most likely due to higher solubility of carbon dioxide and oxygen (Institute of Gas Technology, 1976). The increase in cell potential is caused by the decrease in ohmic polarization losses, and a decrease in activation and concentration polarization. The 29 mV decrease in open-circuit potential can be entirely accounted for the effect of increasing temperature on equilibrium potential. As the temperature increases from 843 to 963°K, the standard electrode potential, E^0, decreases from 1.044 V to 1.009 V, a difference of approximately 35 mV. The contribution of the Nernst term in the open-circuit potential is a net increase of approximately 5 mV as the temperature increases from 843 to 963°K. Thus, the overall change as the temperature rises to 963°K is a decrease in open-circuit potential of close to 30 mV.

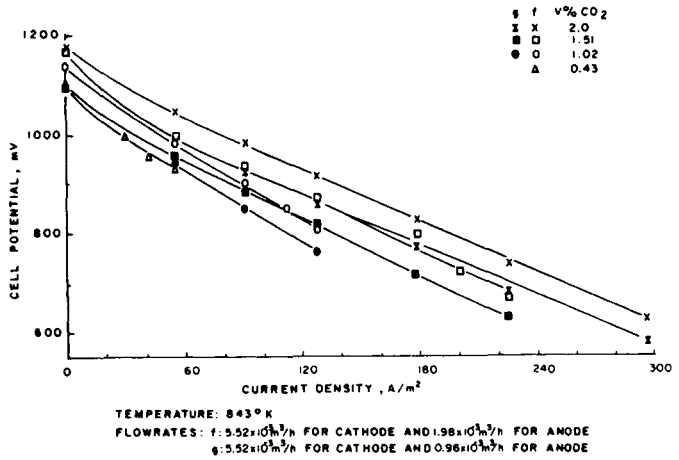

Figure 11. Comparison of cell performance.

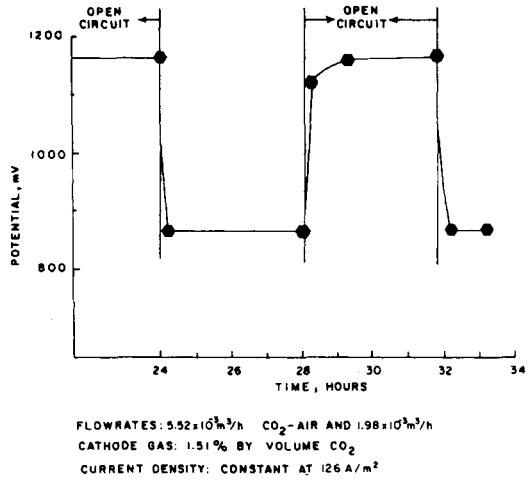

Figure 12. Open-circuit performance on the cell.

Effect of Humidified Gases on Cell Performance. Experimentally, the presence of water in the cathode process gas does not affect the carbon dioxide transfer rate. Also, neither carbon monoxide nor hydrogen is present in the cathode outlet. The outlet of the cathode was analyzed with the carbon monoxide analyzer which indicated zero carbon monoxide (<1 PPM). (See also Discussion section.)

The effect of water vapor on the water-gas shift reaction occurring at the anode can be analyzed using the CO analyzer. Insignificant amounts of carbon monoxide were detected in the anode outlet gas, indicating that the presence of water in the fuel inlet helps to shift equilibrium of the water-gas shift reaction over the C18-HC catalyst. The end result of this equilibrium shift is the production of carbon dioxide and hydrogen.

The results for hydrogen mode operation are summarized qualitatively in Table 1.

Anodic CO_2 Concentration. Although one of the purposes of the device is to produce a concentrated CO_2-H_2 stream at the anode, the IR analyzer permitted direct measurement only to 2.5% CO_2. Anodic conditions during operation will be very similar to that in a molten carbonate fuel cell where high CO_2 concentrations typically exist. Further, in the small test cell very low hydrogen flows would be needed to develop high CO_2 concentrations. The cathodic conditions are quite different from that in a fuel cell; the

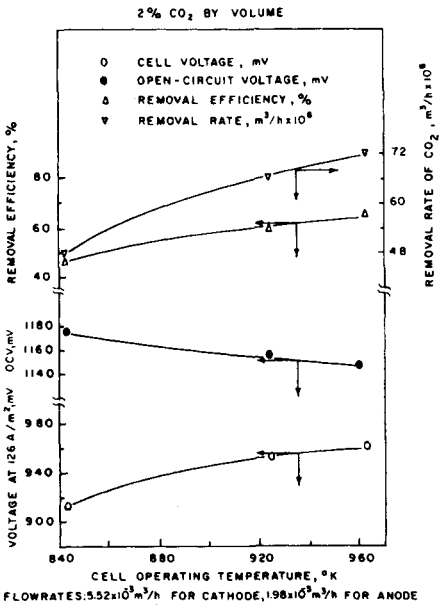

Figure 13. Effect of temperature on cell performance.

TABLE 1. EFFECTS OF OPERATING PARAMETERS

Independent					Dependent			
T (°K)	i_2 (A/m)	H_2 Rate (m^3/h)	Air-CO_2 (m^3/h)	P_{CO_2} (Pa)	E (mV)	N_{CO_2} (m^3/h)	Eff_R (%)	Eff_I (%)
↑	—	—	—	—	↓	↑	↑	↓
—	↑	—	—	—	↓	↑	—	—
—	—	↑	—	—	↓	↑	↓	↑
—	—	—	↑	—	↓	↑	↓	↑
—	—	—	—	↑	↓	↑	↓	↑

↑ Increase
↓ Decrease

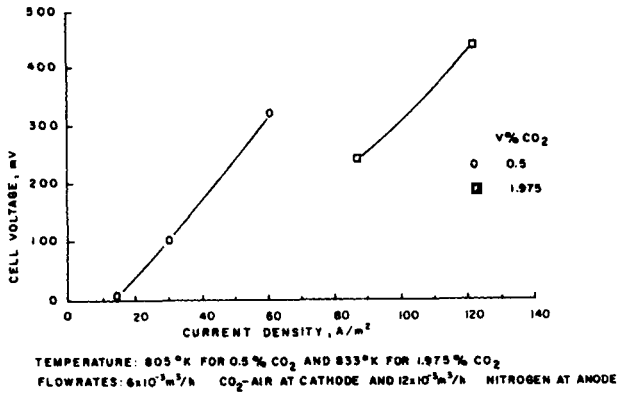

Figure 14. Effect of cell voltage on current density.

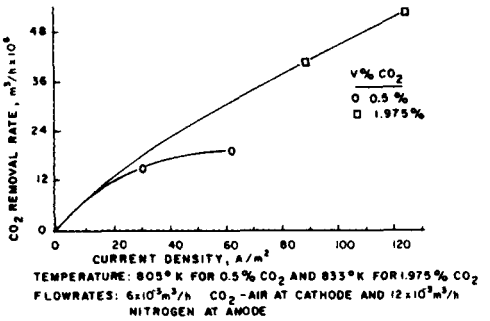

Figure 15. Effect of current on CO_2 removal rate.

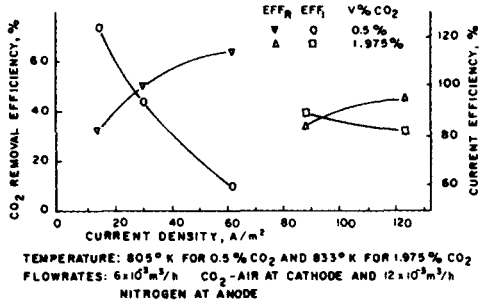

Figure 16. Effect of current on cell performance.

CO_2 levels are as much as two orders of magnitude lower. Thus, attention was focused on the operation at the cathode.

The effluent anodic CO_2 concentrations were normally maintained near 2%. Occasionally, the anodic flow was lowered and the effluent diluted with nitrogen before admission to the analyzer. CO_2 levels in the anode up to about 10% were measured in this manner. A small voltage penalty was noticed, as shown in Figure 11.

Nitrogen Mode

For the nitrogen mode, the cell behavior is similar to the behavior under hydrogen mode operation, with the exception of the dependence of cell voltage on the current density. As seen in Figure 14, the cell voltage increases with increasing current density. This is typical behavior for a driven cell. As the cell current density increases, the carbon dioxide removal rate also increases (Figure 15). The removal efficiency likewise increases with increasing current density (Figure 16). The employment of a recycle at the cathode enhanced the removal performance. Values for the current efficiency are of desirable magnitude. The current efficiency decreases as the applied current density is increased (Figure 16).

DISCUSSION

Calculation of Rate Processes

The concentration of carbon dioxide from the cathode to the anode in an electrochemical concentrator can be described by a series of transport processes. These processes are:

1) Mass transfer through the cathode gas film, governed by: $N = k_g A \Delta c$
2) Diffusion through cathode electrode:

$$N = \frac{DA\epsilon}{\tau}\frac{\Delta c}{\Delta x}$$

3) Reaction of cathode-electrolyte interface
4) Electrolytic transport
5) Reaction at anode-electrolyte interface
6) Diffusion through anode electrode
7) Mass transfer through anode gas film

Calculation of the mass transfer rate permitted by processes (1) and (7) requires knowledge of the gas-phase mass transfer coefficients, k_g. These coefficients can be calculated by using an empirical correlation or experimentally determined using the limiting slope at low P_{CO_2}.

At low carbon dioxide partial pressures, diffusion of carbon dioxide to the cathode is the rate controlling step. Assuming laminar flow across a flat plate, the mass transfer coefficient, k_g, can be expressed empirically (e.g., Bennett and Myers, 1974);

$$k_g = 0.66\frac{D}{L}(\mathrm{Re}_L)^{1/2}(\mathrm{Sc})^{1/3} \qquad (17)$$

The experimental value of k_g is estimated from the limiting slope. The carbon dioxide partial pressure at the reaction interface was assumed to be zero and hence, the driving force for the system is the inlet CO_2 partial pressure.

Calculated k_g

For the cathode gas film:

$D_{CO_2\text{-Air}} = 9.7 \times 10^{-5}$ m^2/s
$A = 6.45 \times 10^{-5}$ m^2 (Figure 3)
$L = 0.032$ m
$U = 0.067$ m/s

$$\mathrm{Re}_L = \frac{LU\rho}{\mu} = 23.8$$

$$\mathrm{Sc} = \mu/\rho D_{CO_2\text{-Air}} = 0.92$$

$$k_g = 0.66 \frac{D_{CO_2\text{-Air}}}{L} (Re_L)^{1/2} (Sc)^{1/3} = 9.4 \times 10^{-3} \text{ m/s}$$

Limiting Slope Method (Experimental)

$\Delta N_{CO_2} = 3.33 \times 10^{-9}$ m^3/s (at 298°K)
$\Delta P_{CO_2} = 200$. Pa (Figure 10)
$A_e = 7.92 \times 10^{-4}$ m^2
$k_g = 6.9 \times 10^{-3}$ m/s (at 923°K)

The two values for k_g, calculated and experimental, agree reasonably well considering the fact that the low P_{CO_2} region has not been adequately investigated. The experimental slope is very approximate.

Tortuosity of Electrode

Diffusion through the porous cathode and anode, processes 2 and 6, is described by:

$$N = \frac{DA\epsilon}{\tau} \frac{\Delta c}{\Delta x}$$

Tortuosity, τ, is a function of electrode geometry. It can be estimated by finding the limiting removal rate (the rate where increasing the oxidant velocity does not increase the removal rate for each P_{CO_2}). At that rate all variables are known with the exception of τ. Tortuosity should be the same for each value of P_{CO_2}. Using Figure 9, for gas compositions of 1.02 V% and 1.51 V% CO_2, τ can be estimated.

Assume that P_{CO_2} at the electrode-electrolyte interface is zero, and that partial pressure at the electrode-gas interface is equal to the log mean average of the inlet and outlet CO_2 concentrations.

Inlet CO_2 Conc. (V%)	Outlet CO_2 Conc. (V%)	Air-CO_2 Flow Rate (m^3/h)	CO_2 Removal Rate (m^3/h)	P_{lm} (%)
1.02	0.613	11.2×10^{-3}	4.6×10^{-5}	0.8
1.51	1.08	11.6×10^{-3}	5.0×10^{-5}	1.28

$\tau_{1.02\ V\%} = 18$.
$\tau_{1.51\ V\%} = 26$.

These two values of tortuosity agree within experimental error.

The anodic and cathodic reactions, electrolytic transport (Processes 3–5) and gas evolution at the anode are presumed to occur fast compared to processes 1 and 2. The molten carbonate fuel cell (e.g., Institute of Gas Technology, 1979) operates at much higher current densities, 1500. A/m^2 and higher. The basic difference between the concentrator and the fuel cell is the CO_2 pressure at the cathode. Thus, these steps (3, 4, 5, 6, 7) are probably near equilibrium at our low current densities.

More sophisticated models, involving several empirical parameters, have been developed for the molten carbonate fuel cell (e.g., Wilemski, 1980). However, in our case, where the control is clearly at the cathode and with the limited data available it does not seem application of such models would be fruitful.

Carbon Monoxide Formation

The absence of carbon monoxide at the cathode can be predicted from thermodynamics. The mixture of air-CO_2 and water vapor at 843°K equilibrates in accordance with the following reaction scheme:

$$CO_{(g)} + {}^1/_2 O_{2(g)} \overset{K_{P_1}}{\rightleftharpoons} CO_{2(g)} \tag{18}$$

$$CO_{(g)} + H_2O_{(g)} \overset{K_{P_2}}{\rightleftharpoons} CO_{2(g)} + H_{2(g)} \tag{19}$$

$${}^1/_2 O_{2(g)} + H_{2(g)} \overset{K_{P_3}}{\rightleftharpoons} H_2O_{(g)} \tag{20}$$

The equilibrium constants for the shift reactions (18) through (20) are 9.266×10^{12}, 3.067, and 3.02×10^{12}, respectively (United Catalysts, Inc., 1979), and the corresponding expressions for K can be written in the following manner:

$$K_{P_1} = 9.266 \times 10^{12} = \frac{P_{CO_2}}{P_{CO}\, P_{O_2}^{1/2}} \times P_T^{-1/2} \tag{21}$$

$$K_{P_2} = 3.067 \times 10^{0} = \frac{P_{CO_2}\, P_{H_2}}{P_{CO}\, P_{H_2O}} \tag{22}$$

$$K_{P_3} = 3.02 \times 10^{12} = \frac{P_{H_2O}}{P_{H_2}\, P_{O_2}^{1/2}} \times P_T^{-1/2} \tag{23}$$

The inlet process gas composition is: $P_{CO_2} = 2.0$ kPa, $P_{H_2O} = 2.2$ kPa, and $P_{O_2} = 20.8$ kPa ($P_{total} = 101.3$ kPa). Substitution of these partial pressures in Eq. 21 yields:

$$P_{CO} = 4.84 \times 10^{-13} \text{ kPa}$$

The equilibrium partial pressure of hydrogen can be found using Eq. 22:

$$P_{H_2} = 1.63 \times 10^{-12} \text{ kPa}$$

Therefore, equilibration at 843°K for this reaction scheme does not allow the formation of either carbon monoxide or hydrogen in the cathode chamber.

ACKNOWLEDGMENT

We wish to thank the National Aeronautics and Space Administration for their financial support through grant NAS 2193. We are also indebted to the Argonne National Laboratory of the DOE, the Institute of Gas Technology, and the General Electric Company for technical advice and supply of electrolyte tiles.

NOTATION

a = activity
A_e = geometric electrode area
c = concentration
D = diffusivity
e = electron
E = equilibrium potential
E^0 = standard state potential
Eff_I = current efficiency
Eff_R = removal efficiency
F = Faraday's constant
i = current density
I = current
K_p = reaction equilibrium constant
k_g = gas-phase mass-transfer coefficient
L = length of flow path
M = gas flow rate
MW = molecular weight
N = removal rate
P = pressure
R = universal gas constant
Re = Reynold's number
Sc = Schmidt number
T = temperature
V% = volume percent

Greek Letters

Δ = change
μ = viscosity
ρ = density
ϵ = porosity
τ = tortuosity

Subscripts

A = anode

C = cathode
g = gas
l = liquid
lm = log mean

LITERATURE CITED

Abdel Salam, O. E., and J. Winnick, "Simulation of an Electrochemical Carbon Dioxide Concentrator," *AIChE J.*, **22**, 1042 (1976).

Argonne National Laboratory, Contract W-31-109-Eng-38, Report No. ANL-77-29 (March, 1977).

Bennett, C. O., and J. E. Myers, "Momentum, Heat and Mass Transfer," 2nd ed., McGraw-Hill, New York, p. 540 (1974).

Degobert, P., and O. Bloch, "Les carbonates alcalins fondus comme electrolytes de piles a combustibles. Metaux susceptibles de servir d'electrodes, "*Bull. Soc. Chim.*, France, 1887 (1962).

Institute of Gas Technology, "Fuel Cell Research on Second Generation Molten Carbonate Systems. Volume II Characteristics of Carbonate Melts," Project 8984 Quarterly Status Report (October to December, 1976).

Institute of Gas Technology, "Fuel Cell Research on Second Generation Molten Carbonate Systems," Project 9105 Final Technical Report, October 1, 1977, through September 30, 1978 (April, 1979).

Kerridge, D. H., "Recent Advances in Molten Salts as Reaction Media," *Pure Appl. Chem.*, **41**, 335 (1975).

Ksenzhek, O. S., "Mechanism of the Functioning of Porous Electrodes," *Fuel Cells: Their Electrochemical Kinetics*, Institute of Electrochemistry, Academy of Sciences of the U.S.S.R., **1**, Consultants Bureau, New York (1966).

Life Systems, Inc., "Technological Advancement of the Electrochemical CO_2 Concentrating Process," NAS CR152250 (May, 1979).

Lin, C. H., and J. Winnick, "An Electrochemical Device for Carbon Dioxide Concentration II. Steady State Analysis CO_2 Transfer," *Ind. Eng. Chem. Process Design Develop.*, **13**, 63 (1974).

Sribnik, F., and W. C. Dean, "*Hydrogen Depolarized Cell Water Vapor Electrolysis Cell:* CO_2 Collection Subsystem Preliminary Design Package," SSP Document Number A35, Hamilton Standard, Windsor Locks, CN (May, 1971).

Stepanov, G. K., and A. M. Trunov, "Electroreduction of Oxygen in Molten Carbonates, "*Electrochemistry of Molten and Solid Electrolytes*," U.S.S.R., **3**, 74, Consultants Bureau, New York (1966).

Swaroop, R. B., J. W. Sim, and K. Kinoshita, "Corrosion Protection of Molten Carbonate Fuel Cell Gas Seals," *J. Electrochem. Soc.*, **125**, 1799 (1978).

United Catalysts, Inc., "Physical and Thermodynamic Properties of Elements and Compounds," Louisville, KY.

Vogel, W. M., L. J. Bregoli, and Smith, S. W., "Electrochemical Oxidation of H_2 and CO in Fused Alkali Metal Carbonates," *J. Electrochem. Soc.*, **127**, (4), 883 (1980).

Wilemski, G., Final Report No. DE-AC-03-79ET11322 (July, 1979).

Winnick, J., R. D. Marshall, and F. H. Schubert, "An Electrochemical Device for Carbon Dioxide Concentration I. System Design and Performance," *Ind. Eng. Chem. Process Design Develop.*, **13**, 59 (1974).

Winnick, J. and P. Ross, "Kinetics of O_2, CO_2 Reduction at the Molten Carbonate Fuel Cell Cathode," *J. Electrochem. Soc.* **128**, 991 (1981).

Manuscript received August 28, 1980; revision received February 18 and accepted March 4, 1981.

The Rheological Characterization of Coal Liquefaction Preheater Slurries

Rheological characterizations were made for a coal liquefaction preheater slurry; measurements were made in line at high temperature and high pressure. Above 400°K, the coal-solvent slurry (35 wt. % coal) was pseudoplastic and was adequately modeled by a power-law equation. Experimental data over a temperature range of 400 to 700°K were correlated, and critical slurry velocities for transition from laminar flow were calculated for flow in several pipe diameters.

J. R. THURGOOD, R. W. HANKS, G. E. OSWALD, and E. L. YOUNGBLOOD

Oak Ridge National Laboratory
Oak Ridge, TN 37830

SCOPE

The rheological characterization of coal-solvent slurries in liquefaction preheaters has received little attention because of the difficulties encountered in making measurements under severe process conditions. The usual approach in collecting rheological data on preheater slurries has been to take measurements on autoclave samples that have been reduced in pressure and temperature. The results are then extrapolated to the process temperature and pressure by means of correlations developed mainly for the petroleum industry. Few measurements have been made at actual process conditions to verify the use of such procedures. Basic rheological data are essential to ensure optimum design of the large demonstration plant preheaters presently under consideration.

The objective of the present work is to present a method for collecting rheological data for coal-solvent slurries at high pressure and high temperature. Measurements are made in line with a capillary-tube or pipeline viscometer. Experimental results and an empirical data correlation are presented for slurries at high pressure and at several temperatures. These results are expected to be particularly helpful in establishing the effects of rheology on heat transfer correlations and in providing basic data for proper multiphase flow regime mapping of the preheating process.

CONCLUSIONS AND SIGNIFICANCE

Rheological characterizations of a coal-solvent slurry containing 35 wt. % coal were made at a pressure of 13.9 MPa and at temperatures ranging from 400 to 700°K. Rheograms (shear-stress versus shear-rate plots) of the slurry at four different temperatures are shown in Figure 7. An empirical correlation between temperature-corrected shear stress and $8V/D$ was developed that allowed correlation of the data with a standard deviation of 3.6%. Critical velocities for the change of flow type from laminar to transitional were calculated for the slurry in

J. R. Thurgood is now with Utah Power and Light Co., P.O. Box 899, Salt Lake City, Utah 84110.

R. W. Hanks is Chairman of the Department of Chemical Engineering, Brigham Young University, Provo, Utah 84601.

Correspondence concerning this paper should be addressd to E. L. Youngblood.